

Thermal C–P and C–H cleavage in co-ordinated phosphines leading to dinuclear platinum complexes and contrasting reactions with $M(\text{PPh}_3)^+$ ($M = \text{Cu}, \text{Ag}$ or Au) and HgCl_2^\dagger

Robert Bender,^{*a} Salah-Eddine Bouaoud,^b Pierre Braunstein,^{*a} Yves Dusausoy,^c
 Naima Merabet,^b Jesus Raya^d and Djamil Rouag^b

^a Laboratoire de Chimie de Coordination, UMR 7513 CNRS, Université Louis Pasteur, 4 rue Blaise Pascal, F-67070 Strasbourg Cédex, France. E-mail: braunst@chimie.u-strasbg.fr

^b Institut de Chimie, Université de Constantine, Route de Ain el Bey, Constantine, Algeria

^c Laboratoire de Cristallographie et Modélisation des Matériaux Minéraux et Biologiques, UPRESA 7036, Université Henri Poincaré, Nancy I, Faculté des Sciences, Boîte postale 239, F-54506 Vandoeuvre-les-Nancy, France

^d UMR 50 CNRS-ULP-Bruker, Université Louis Pasteur, 4 rue Blaise Pascal, F-67070 Strasbourg Cédex, France

Received 3rd December 1998, Accepted 20th January 1999

The dinuclear complex $[\text{Pt}_2(\mu\text{-PPh}_2)\{\mu\text{-}(o\text{-C}_6\text{H}_4\text{PPh}_2)\}(\text{PPh}_3)_2]$ was prepared by controlled thermolysis of $[\text{Pt}(\text{C}_2\text{H}_4)(\text{PPh}_3)_2]$ and it contains both a diphenylphosphido and an *ortho*-metallated triphenylphosphine ligand that bridge the Pt–Pt bond [2.657(1) Å in **3** and 2.677(5) Å in the CH_2Cl_2 adduct]. Addition of the electrophilic metal reagents $[\text{M}(\text{PPh}_3)]^+$ ($M = \text{Cu}, \text{Ag}$ or Au) occurs at the Pt–Pt bond, affording $[\text{Pt}_2\{\mu\text{-M}(\text{PPh}_3)\}(\mu\text{-PPh}_2)\{\mu\text{-}(o\text{-C}_6\text{H}_4\text{PPh}_2)\}(\text{PPh}_3)_2]^+$ ($M = \text{Cu}, \text{Ag}$ or Au) whereas selective oxidation by HgCl_2 gives the dinuclear platinum(II) complex $[\text{Pt}_2\text{Cl}_2(\mu\text{-PPh}_2)\{\mu\text{-}(o\text{-C}_6\text{H}_4\text{PPh}_2)\}(\text{PPh}_3)_2]$ which is shown to have a “mixed-geometry” structure at the metal centres (square planar and flattened tetrahedral). The new complexes have been analysed by $^{31}\text{P}\text{-}\{^1\text{H}\}$ and ^{195}Pt NMR spectroscopy and the structures of three complexes have been determined by X-ray diffraction.

The structure and reactivity of platinum complexes with only phosphorus-containing ligands are still poorly understood, notwithstanding the fact that the first platinum zerovalent compounds $[\text{Pt}(\text{PPh}_3)_3,4]$ were discovered *ca.* 40 years ago.¹ It became rapidly evident that the complexity of their solution chemistry is largely due to the easy occurrence of complex thermal transformations. Indeed, tertiary phosphine complexes are liable to undergo C–H or C–P bond cleavage depending on the specific reaction conditions that they are exposed to. Such reactions have profound implications in organometallic chemistry and homogeneous catalysis, owing to the ubiquitous role of these ligands.² Whereas it has long been observed that red solutions are produced upon thermolysis of these and related platinum complexes in organic solvents, their composition is only partly known or controversial, and detailed structural information is lacking, with the exceptions of $[\text{Pt}_2(\mu\text{-PPh}_2)_2(\text{PPh}_3)_2]$ **1** and $[\text{Pt}_3\text{Ph}(\mu\text{-PPh}_2)_3(\text{PPh}_3)_2]$ **2** which obviously result from C–P cleavage reactions of co-ordinated PPh_3 . The latter complex is remarkable in that it can adopt at least four isomeric structures in the solid state, depending on the recrystallization solvent used.^{3–6}

Polynuclear complexes containing phosphido or *ortho*-metallated $o\text{-C}_6\text{H}_4\text{PPh}_2$ bridges can result from C–P or C–H cleavage reactions of co-ordinated PPh_3 , respectively.² Here we

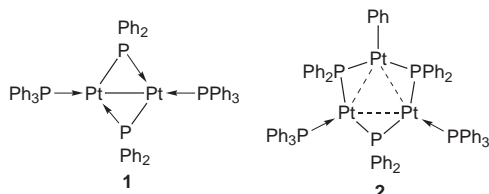
show that a dinuclear platinum complex, $[\text{Pt}_2(\mu\text{-PPh}_2)\{\mu\text{-}(o\text{-C}_6\text{H}_4\text{PPh}_2)\}(\text{PPh}_3)_2]$ **3**, containing both types of 3-electron donor bridges is also formed in such reactions. Its metal–metal bond is electron rich and adducts with electrophilic reagents $[\text{M}(\text{PPh}_3)]^+$ ($M = \text{Cu}, \text{Ag}$ or Au) have been isolated whereas selective oxidation by HgCl_2 yields a platinum(II) dinuclear complex having an unusual structure. The new complexes **3–6** described in this paper were characterized by ^{195}Pt and $^{31}\text{P}\text{-}\{^1\text{H}\}$ NMR spectroscopy; ^{195}Pt NMR establishes unambiguously the bonding between the Pt atoms in these complexes. We determined the crystal structure of **3** in 1988 and presented preliminary results in 1993.⁷

Results and discussion

1 Synthesis, crystal structure and NMR study of $[\text{Pt}_2(\mu\text{-PPh}_2)\{\mu\text{-}(o\text{-C}_6\text{H}_4\text{PPh}_2)\}(\text{PPh}_3)_2]$ **3**

Heating solutions of platinum(0) complexes such as $[\text{Pt}(\text{PPh}_3)_3,4]$ in solvents like acetone, benzene or toluene affords red solutions which contain amongst others $[\text{Pt}_2(\mu\text{-PPh}_2)_2(\text{PPh}_3)_2]$ **1** and the cluster $[\text{Pt}_3\text{Ph}(\mu\text{-PPh}_2)_3(\text{PPh}_3)_2]$ **2**.^{3,5} We repeated these thermolysis experiments a number of times under different experimental conditions and this convinced us that the composition of these red solutions was more complex than originally thought. In order to improve the yields of complexes which like **1** and **2** have a P:Pt ratio equal or near to 2:1 we have used $[\text{Pt}(\text{C}_2\text{H}_4)(\text{PPh}_3)_2]$ as a starting material, eqn. (1).

However, when 2-methoxyethanol was chosen as solvent for the reaction we observed that formation of complex **1** was suppressed and this could therefore lead to an increased yield of **3**. After refluxing a 2-methoxyethanol solution of $[\text{Pt}(\text{C}_2\text{H}_4)(\text{PPh}_3)_2]$ at 70 °C under nitrogen for 4 h the red cluster $[\text{Pt}_3\text{Ph}(\mu\text{-PPh}_2)_3(\text{PPh}_3)_2]$ **2** precipitated directly in *ca.* 35% yield and the yellow complex $[\text{Pt}_2(\mu\text{-PPh}_2)\{\mu\text{-}(o\text{-C}_6\text{H}_4\text{PPh}_2)\}(\text{PPh}_3)_2]$ **3** was isolated from the solution in 35–40% yield (based on platinum).



[†] Dedicated to Professor M. I. Bruce on the occasion of his 60th Birthday, with our warmest congratulations and best wishes.

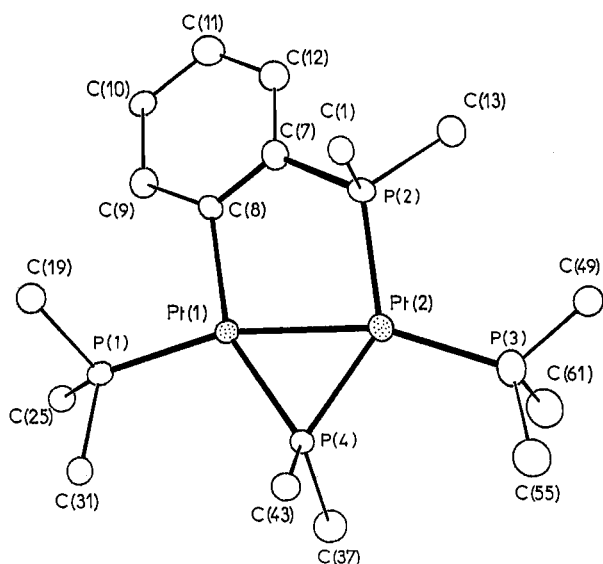
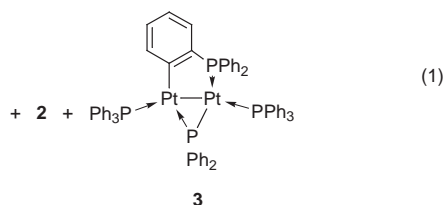
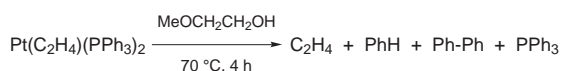


Fig. 1 View of the structure of $[\text{Pt}_2(\mu\text{-PPh}_2)\{\mu\text{-}(o\text{-C}_6\text{H}_4\text{PPh}_2)\}(\text{PPh}_3)_2]$ **3**. For sake of clarity, the C_6H_5 groups bound to the phosphorus atoms are represented by their *ipso*-carbons only.



Further work-up of the filtrate led to additional crops of **2** and **3**. Separation of these complexes was based on their difference of solubility: **3** is easily soluble in a large variety of organic solvents, while **2** is only sparingly soluble in most of them, but more soluble in CH_2Cl_2 , where it decomposes however after several days.⁸ In addition, the reaction mixture contains benzene as determined by GPC, and two compounds isolated in the solid state, biphenyl and OPPh_3 . The latter results from the air oxidation of the PPh_3 liberated during the thermolysis. The IR spectrum (KBr pellet) of complex **3** shows a band at 725 cm^{-1} , characteristic of *ortho*-metallation (see below).^{9–11}

Crystal structures. The single crystal X-ray analysis established that **3** is a dinuclear complex with a $\text{Pt}^{\text{I}}\text{-Pt}^{\text{I}}$ $d^9\text{-d}^9$ metal-metal bond, bridged by both a $\mu\text{-PPh}_2$ and a $\mu\text{-}(o\text{-C}_6\text{H}_4\text{PPh}_2)$ group (Fig. 1). Selected bond distances and angles are given in Table 1. The resulting three and five membered rings as well as the P atoms of the terminal phosphines are almost coplanar. The largest deviation from the mean plane through Pt(1), Pt(2), P(1), P(2), P(3), P(4), C(7) and C(8) is that of P(2) (-0.646 \AA). The Pt-Pt distance of $2.657(1)\text{ \AA}$ is somewhat longer than in the related, symmetrical dinuclear platinum(II) complexes $[\text{Pt}_2(\mu\text{-PPh}_2)_2(\text{PPh}_3)_2]$ **1** [$2.604(1)\text{ \AA}$]³ and $[\text{Pt}_2\{\mu\text{-}(o\text{-C}_6\text{H}_4\text{PPh}_2)\}_2(\text{PPh}_3)_2]$ [$2.630(1)\text{ \AA}$].⁹ The Pt-P distances around Pt(2) are slightly longer than those around the less crowded Pt(1) atom, but these values are in the range observed in similar complexes.^{3,5,9} The Pt(1)-P(4)-Pt(2) angle [$71.4(2)^\circ$] is rather small for bridging phosphido groups when compared with those of both isomers of **2**.⁵ The terminal phosphines are slightly bent towards P(4) and the *ortho*-metallated phosphine deviates slightly from the orthogonality to the Pt-Pt vector.

Cycloplatinated products have been previously claimed from similar thermolysis reactions,^{10–12} but owing to lack of structural information it could not be established whether the com-

Table 1 Selected bond distances (\AA) and angles ($^\circ$) in complexes **3** and **3** $\cdot\text{CH}_2\text{Cl}_2$

	3	3 $\cdot\text{CH}_2\text{Cl}_2$
Pt(1)-Pt(2)	2.657(1)	2.677(5)
Pt(1)-C(1)	2.11(2)	2.094(8)
Pt(1)-P(1)	2.224(6)	2.239(2)
Pt(1)-P(4)	2.255(6)	2.247(2)
Pt(2)-P(2)	2.274(7)	2.265(2)
Pt(2)-P(3)	2.30(1)	2.285(2)
Pt(2)-P(4)	2.296(2)	2.281(2)
Pt(2)-C(7)	1.76(2)	1.802(9)
C(7)-C(8)	1.40(3)	1.40(1)
P(1)-Pt(1)-Pt(2)	163.0(1)	161.19(6)
P(1)-Pt(1)-C(8)	98.5(5)	100.1(2)
P(1)-Pt(1)-P(4)	108.1(2)	109.50(8)
Pt(1)-P(4)-Pt(2)	71.4(2)	72.18(7)
Pt(1)-Pt(2)-P(2)	83.4(2)	80.30(6)
Pt(1)-Pt(2)-P(3)	160.6(3)	164.65(6)
Pt(1)-Pt(2)-P(4)	53.6(2)	53.32(6)
P(2)-Pt(2)-P(3)	114.4(3)	114.45(8)
P(2)-Pt(2)-C(7)	112.5(8)	113.6(3)
P(2)-C(7)-C(8)	124(2)	115.5(6)
C(7)-C(8)-Pt(1)	114(1)	117.8(6)
C(8)-Pt(1)-Pt(2)	98.5(5)	97.4(2)
C(8)-Pt(1)-P(4)	153.2(5)	149.5(2)

plexes contained a four-membered ring or the 1,3 difunctional bridging ligand found in **3**. Furthermore, there seems to exist only one well established example of cycloplatinated of PPh_3 ,¹³ although indirect access to related systems has been described recently.^{9,14}

Having previously experienced with platinum clusters the chemical or structural consequences of changing crystallization solvents,^{4,5} we recrystallized complex **3** by slow diffusion of a mixture of hexanes into a solution of it in CH_2Cl_2 . This afforded new crystals of **3** $\cdot\text{CH}_2\text{Cl}_2$ with different cell parameters. However, the molecular structure of **3** $\cdot\text{CH}_2\text{Cl}_2$ is almost identical to that of **3**. Only a few angles differ slightly on going from **3** to **3** $\cdot\text{CH}_2\text{Cl}_2$. The largest difference lies in the deviation of the skeleton atoms from the mean plane calculated for each molecule. The P(2) atom of the *ortho*-metallated ligand lies on one side of the mean plane in **3** (0.646 \AA) and on the opposite side (-0.627 \AA) in **3** $\cdot\text{CH}_2\text{Cl}_2$. This emphasizes the flexibility of the five membered *ortho*-metallated ring in complex **3**. After completion of this paper a report describing the structure of **3** appeared which shows almost identical bonding parameters, slight differences being again observed in the *ortho*-metallated ring.¹⁵ We have independently checked that formation of cluster **2** does not involve the intermediacy of **3** as treatment of the latter complex under conditions known to produce cluster **2** led to its quantitative recovery.

NMR Spectroscopy. Owing to the existence of the isotope ^{195}Pt ($I = 1/2$, natural abundance = 33.8%) a sample of this dinuclear complex contains two chemically different Pt atoms and is constituted by four isotopomers, *i.e.* 43.8% of molecules are without ^{195}Pt , $2 \times 22.4\%$ contain one ^{195}Pt nucleus and 11.4% contain two ^{195}Pt nuclei. The observed spectrum is the superimposition of the spectra of each of these isotopomers, with the intensities taking into account their respective natural abundance.

The ^{195}Pt NMR spectrum of complex **3** presents two groups of 16 intense peaks, where each group represents a ddd centered at $\delta -2837$ [Pt(1)] and -3343 [Pt(2)], respectively, and originates from coupling of each of the chemically different platinum nuclei to the various phosphorus nuclei (see Fig. 2 and Table 2). Each of the 16 peaks is flanked by a doublet, smaller in intensity, due to $^1J(\text{Pt-Pt}) = 1552\text{ Hz}$. The large values of the platinum-phosphorus coupling constants (2116 to 3344 Hz) indicate a $^1J(\text{Pt-P})$ and hence direct Pt(1)-P(1), Pt(1)-P(4),

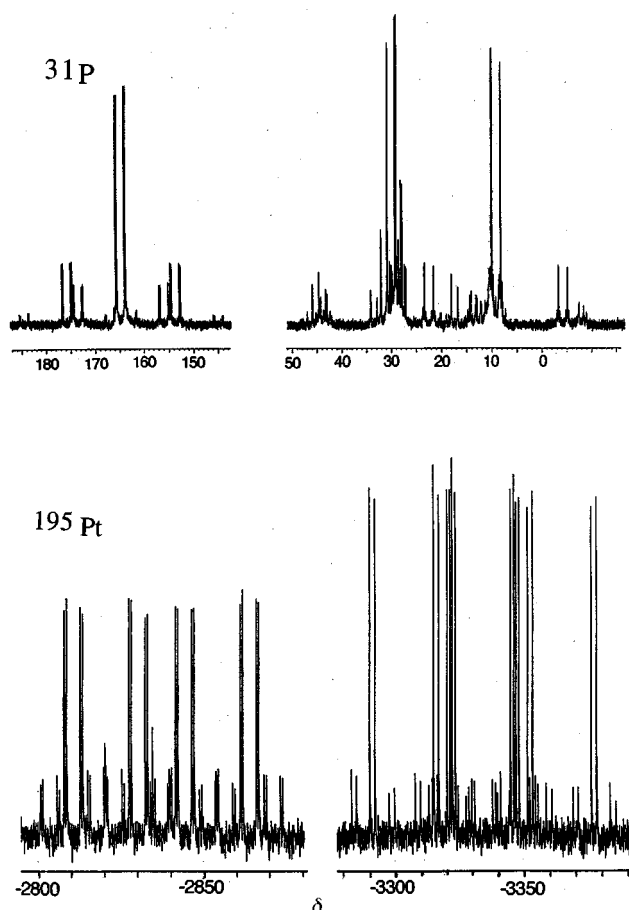


Fig. 2 The ^{195}Pt - $\{^1\text{H}\}$ and ^{31}P - $\{^1\text{H}\}$ NMR spectra (in acetone) of complex $[\text{Pt}_2(\mu\text{-PPh}_2)\{\mu\text{-}(o\text{-C}_6\text{H}_4\text{PPh}_2)\}(\text{PPh}_3)_2]^+$ **3**.

Pt(2)–P(2), Pt(2)–P(3) and Pt(2)–P(4) bonds. The smaller coupling constants (76 to 526 Hz) represent 2 or $^3J(\text{Pt}–\text{P})$ couplings. The reported $^2J(\text{Pt}–\text{P})$ value of 1149 Hz involving the tertiary phosphine ligand of $[\text{Pt}_2\{\mu\text{-}(o\text{-C}_6\text{H}_4\text{PPh}_2)\}_2(\text{PPh}_3)_2]^+$ appears surprisingly high when compared with that of **3**. The ^{31}P - $\{^1\text{H}\}$ NMR spectrum of **3** contains signals for four inequivalent phosphorus nuclei flanked by the satellites due to the platinum–phosphorus couplings. The spectra could be analysed using the first order approximation and spectral simulation using gNMR gave very similar values. Therefore only the absolute values of the coupling constants are reported (Table 2). The most deshielded signal (δ 162.7) with two different pairs of satellites is the resonance of P(4), which bridges both platinum atoms. When compared with the chemical shift of the phosphido ligand in **1** at δ 198.2 [CH_2Cl_2 , t, $^2J(\text{P}–\text{P}) = 55$ Hz],¹⁶ the upfield shift observed is consistent with a slightly shorter metal–metal bond in **1** [2.604(1) Å].^{2,3,17} The $^1J(\text{Pt}–\mu\text{-P})$ values of 2116 and 2646 Hz of **3** should be compared with that of 2773 Hz for **1**. The other signals all correspond to the tertiary phosphines. The resonances at δ 26.6 and 27.6 for P¹ and P³ are upfield to that of δ 44.4 for **1** and their $^1J(\text{Pt}–\text{P})$ coupling constants are significantly smaller than those of **1** (ca. 5200 Hz).¹⁶ This spectrum confirms the $J(\text{Pt}–\text{P})$ values found in the ^{195}Pt NMR spectrum and, in addition, the large values of $J(\text{P}–\text{P})$ reveal the respective *trans* positions of P(1) and P(3) and P(2) and P(4), while the smaller $J(\text{P}–\text{P})$ couplings indicate *cisoid* positions for P(1) and P(3) with respect to P(2) and P(4). Clearly, the molecular structure of complex **3** in the solid state is maintained in solution.

2 Reactivity of complex **3** with the electrophilic fragments $[\text{M}(\text{PPh}_3)]^+$ (M = Cu, Ag or Au)

Complex **3** reacts easily with the electrophiles $[\text{M}(\text{PPh}_3)]^+$ to give the cationic trinuclear clusters $[\text{Pt}_2\{\text{M}(\text{PPh}_3)\}\{\mu\text{-PPh}_2\}]^+$

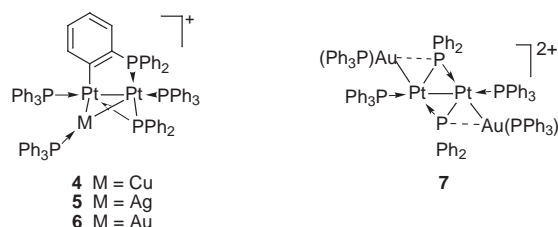
Table 2 Selected ^{195}Pt - $\{^1\text{H}\}$ and ^{31}P - $\{^1\text{H}\}$ NMR data for complexes **3–6** (δ , J/Hz)

3

4 M = Cu
5 M = Ag
6 M = Au

	3	4	5	6
$\delta(\text{Pt}^1)$	–2838	–2847	–2664	–2501
$\delta(\text{Pt}^2)$	–3334	–3060	–3061	–2857
$^1J(\text{Pt}–\text{Pt})$	1552	818	n.d.	815
$^1J(\text{Pt}^1–\text{Ag})$			540, 470	
$^1J(\text{Pt}^2–\text{Ag})$			420, 360	
$\delta(\text{P}^1)$	26.6	33.1	31.1	31.7
$\delta(\text{P}^2)$	7.2	14.6	19.6	25.1
$\delta(\text{P}^3)$	27.6	36.5	34.3	32.9
$\delta(\text{P}^4)$	162.7	187.2	178.6	161
$\delta(\text{P}^5)$	—	5.6	13.6	28.9
$^1J(\text{P}^1–\text{Pt}^1)$	3610	3782	3766	3946
$^1J(\text{P}^2–\text{Pt}^2)$	3210	2542	2554	2425
$^1J(\text{P}^3–\text{Pt}^2)$	3344	3550	3550	3754
$^1J(\text{P}^4–\text{Pt}^1)$	2116	2191	1945	1705
$^1J(\text{P}^4–\text{Pt}^2)$	2646	2315	2225	1991
$^2J(\text{P}^1–\text{Pt}^2)$	215	209	198	177
$^2J(\text{P}^2–\text{Pt}^1)$	76	56	54	42
$^2J(\text{P}^3–\text{Pt}^1)$	526	275	300	286
$^2J(\text{P}^5–\text{Pt}^1)$	—	n.d.	n.d.	439
$^2J(\text{P}^5–\text{Pt}^2)$	—	n.d.	n.d.	372
$^3J(\text{P}^1–\text{Ag})$	—	—	15	—
$^3J(\text{P}^3–\text{Ag})$	—	—	38	—
$^3J(\text{P}^4–\text{Ag})$	—	—	5	—
$^1J(\text{P}^5–\text{Ag})$	—	—	662, 575	—
$^3J(\text{P}^1–\text{P}^2)$	6	<5	<5	<5
$^3J(\text{P}^1–\text{P}^3)$	151	128	134	112
$^2J(\text{P}^1–\text{P}^4)$	29	17	16	<5
$^3J(\text{P}^1–\text{P}^5)$	—	—	—	25
$^2J(\text{P}^2–\text{P}^3)$	9	<5	<5	<5
$^2J(\text{P}^2–\text{P}^4)$	213	218	220	231
$^2J(\text{P}^3–\text{P}^4)$	<5	<5	<5	<5
$^3J(\text{P}^3–\text{P}^5)$	—	n.d.	5	34

$\{\mu\text{-}(o\text{-C}_6\text{H}_4\text{PPh}_2)\}(\text{PPh}_3)_2]^+$ (M = Cu **4**, Ag **5** or Au **6**) in which the $[\text{M}(\text{PPh}_3)]^+$ fragment, which is isolobal to the proton, has been added to the metal–metal bond of **3**, in a bridging position. The Pt atoms are now linked by three chemically different bridging groups.



It is interesting to recall that addition of $[\text{Au}(\text{PPh}_3)]^+$ to complex **1** afforded the unusual dicationic tetranuclear cluster $[\text{Pt}_2\text{Au}_2(\mu\text{-PPh}_2)_2(\text{PPh}_3)_4]^{2+}$ **7** with an original hammock-like structure. In this complex each $[\text{Au}(\text{PPh}_3)]^+$ fragment is linked to a different Pt atom in a semi-bridging position between the Pt atom and a diphenylphosphido bridge.¹⁸

NMR Spectroscopy of the Pt_2M complexes **4–6.** The ^{31}P - $\{^1\text{H}\}$ and ^{195}Pt NMR spectra of the trinuclear complexes **4–6** are shown in Figs. 3–5 because their complexity is very diagnostic and they illustrate the changes which occur within a series of

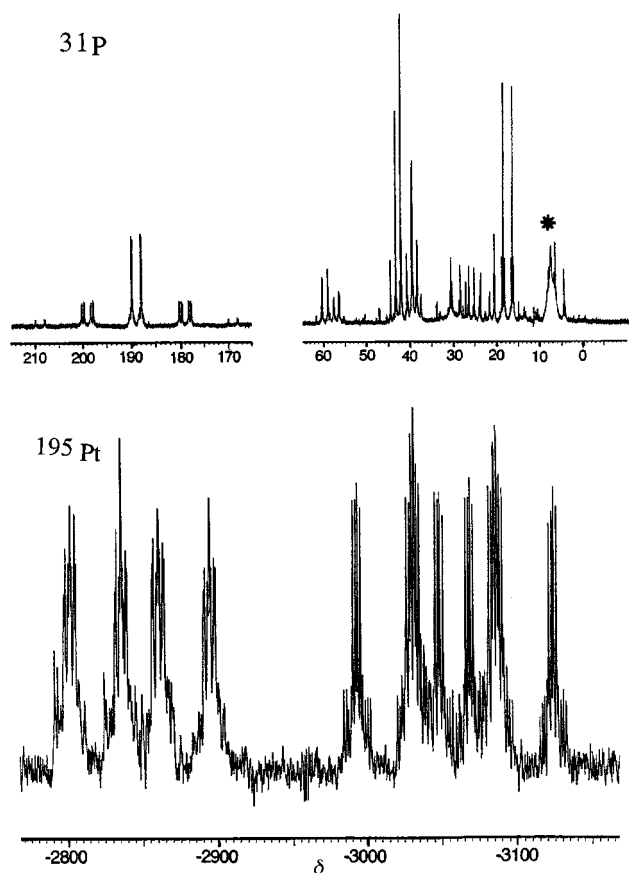


Fig. 3 The $^{195}\text{Pt}\{-^1\text{H}\}$ and $^{31}\text{P}\{-^1\text{H}\}$ NMR spectra (in acetone) of the cationic complex $[\text{Pt}_2\{\mu\text{-Cu}(\text{PPh}_3)\}_2\{\mu\text{-PPH}_2\}\{\mu\text{-}(o\text{-C}_6\text{H}_4\text{PPh}_2)\}_2(\text{PPh}_3)_2]^+$ **4**. The asterisk denotes the resonance of the P(5) nucleus bound to Cu.

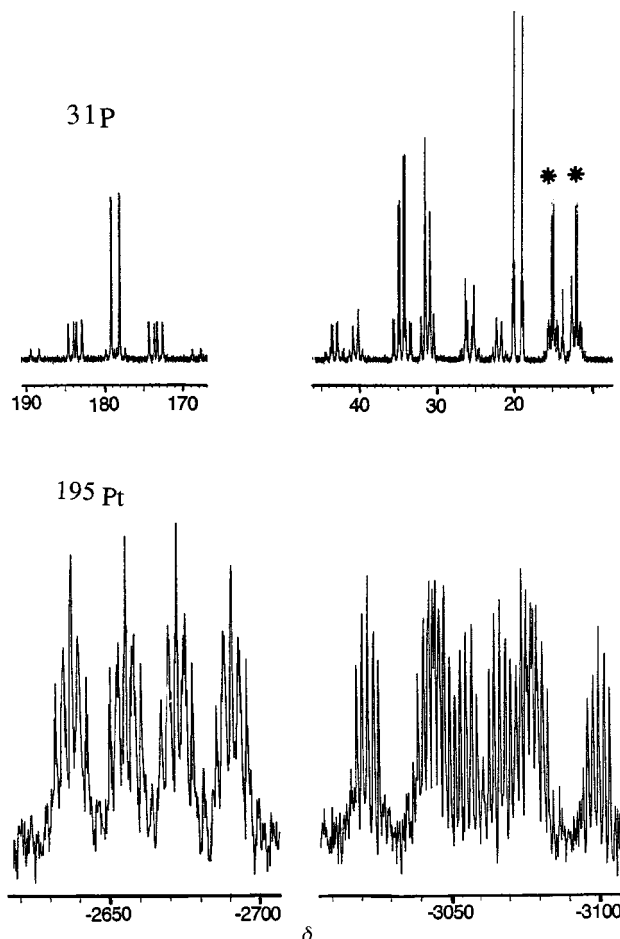


Fig. 4 The $^{195}\text{Pt}\{-^1\text{H}\}$ and $^{31}\text{P}\{-^1\text{H}\}$ NMR spectra (in acetone) of the cationic complex $[\text{Pt}_2\{\mu\text{-Ag}(\text{PPh}_3)\}_2\{\mu\text{-PPH}_2\}\{\mu\text{-}(o\text{-C}_6\text{H}_4\text{PPh}_2)\}_2(\text{PPh}_3)_2]^+$ **5**. The asterisks denote the resonances of the P(5) nucleus bound to Ag.

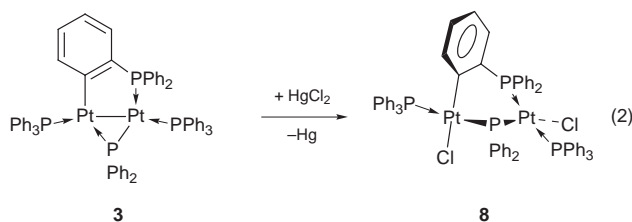
closely related molecules. These spectra could be analysed using the first order approximation. The addition of $[\text{M}(\text{PPh}_3)]^+$ to complex **3** is evidenced in $^{31}\text{P}\{-^1\text{H}\}$ NMR spectroscopy by the presence of an additional signal at δ 5.6 for **4**, 13.6 for **5** and 28.9 for **6**. The four other signals of the $[\text{Pt}_2(\mu\text{-PPH}_2)\{\mu\text{-}(o\text{-C}_6\text{H}_4\text{PPh}_2)\}_2(\text{PPh}_3)_2]$ unit remain roughly unchanged. The new signal shows the couplings of P(5) with Pt(1) and Pt(2) and with phosphorus atoms. In cluster **4** the quadrupole of the Cu atom ($I = 3/2$) transforms the signal of P(5) into a large hump surmounted by a sharper peak at δ 5.6. No coupling constant could be derived from this resonance. For all the Pt_2M^+ clusters, several peaks, with linewidth reaching 28 Hz, hide small coupling constants [$J(\text{P}\text{-P}) < 3\text{-}4$ Hz], which could not be measured on the spectra.

The Ag-bound P(5) in complex **5** appears as two centered doublets (Fig. 4), due to coupling of P(5) with both isotopes ^{107}Ag and ^{109}Ag ($I = 1/2$, natural abundance 51.8 and 48.2%, respectively). For comparison, the $^{31}\text{P}\{-^1\text{H}\}$ NMR spectrum of the platinum–gold complex **6** is shown in Fig. 5.

The ^{195}Pt NMR spectra of clusters **4–6** present a higher multiplicity than that of complex **3**, owing to the additional couplings of both Pt atoms with P(5). Furthermore, the two isotopes of the silver atom in **5** couple with each Pt atom, with $^1J(\text{Ag}\text{-Pt})$ of 540 and 470 Hz for Pt(1) and 420 and 360 Hz for Pt(2), respectively. The various $^2J(\text{Pt}\text{-P}(5))$ and $^1J(\text{Pt}\text{-Ag})$ couplings confirm the co-ordination of the $[\text{M}(\text{PPh}_3)]^+$ fragment in a bridging position between the two Pt atoms. This is also consistent with the decrease of $^1J(\text{Pt}\text{-Pt})$ from 1552 Hz for **3** to *ca.* 815 Hz for **4** and **6** (this coupling constant could not be measured in the ^{195}Pt spectrum of **5**, but it should be of the same magnitude as in **4** and **6**), the deshielding of the P atoms and the displacement of the chemical shift of the Pt atoms towards more positive values.

3 Reaction of complex **3** with HgCl_2 : synthesis, structure and NMR study of $[\text{Pt}_2\text{Cl}_2(\mu\text{-PPH}_2)\{\mu\text{-}(o\text{-C}_6\text{H}_4\text{PPh}_2)\}_2(\text{PPh}_3)_2]$ **8**

Like $[\text{M}(\text{PPh}_3)]^+$ ($\text{M} = \text{Cu}, \text{Ag}$ or Au), HgCl_2 is a Lewis acid that can add to an electron-rich metal–metal bond.¹⁹ Such a complex is probably formed as an unstable intermediate when **3** is treated with HgCl_2 . After a color change occurs from yellow to orange, a slow deposition of Hg^0 is observed and the solution lightens to pale yellow, from which complex **8** was isolated in good yield, eqn. (2). In this reaction both Pt^{I} of complex **3** have



been oxidized to Pt^{II} , with breaking of the metal–metal bond and rearrangement of the skeleton geometry. A similar oxidation and a $\text{Pd}^{\text{I}}\text{-Pd}^{\text{I}}$ bond has been encountered in the reaction of HgCl_2 with $[\text{Pd}_2\text{Cl}_2(\mu\text{-Ph}_2\text{PCH}_2\text{PPh}_2)_2]$.²⁰

In contrast, oxidation of the bis(cyclometallated) complex $[\text{Pt}_2(\mu\text{-}o\text{-C}_6\text{H}_4\text{PPh}_2)_2(\text{PPh}_3)_2]$ by I_2 afforded an ionic complex, where the metal–metal bond has been broken and an iodine atom occupies a bridging position between the two Pt atoms, the second iodine being anionic.⁹

Crystal structure. The molecular structure of complex **8** was determined by single crystal X-ray diffraction (Fig. 6) and

Table 3 Selected bond distances (Å) and angles (°) in complex $[\text{Pt}_2\text{Cl}_2(\mu\text{-PPh}_2)\{\mu\text{-}(o\text{-C}_6\text{H}_4\text{PPh}_2)\}(\text{PPh}_3)_2]^+$ **8**

Pt(1)···Pt(2)	3.596(1)	Cl(1)–Pt(1)–C(30)	177.2(6)
Pt(1)–Cl(1)	2.373(6)	C(30)–Pt(1)–P(4)	86.1(6)
Pt(1)–C(30)	2.09(2)	P(1)–Pt(1)–P(4)	177.8(2)
Pt(1)–P(1)	2.331(6)	P(1)–Pt(1)–Cl(1)	86.5(2)
Pt(1)–P(4)	2.326(6)	P(1)–Pt(1)–C(30)	92.0(5)
Pt(2)–Cl(2)	2.378(6)	Cl(1)–Pt(1)–P(4)	95.4(3)
Pt(2)–P(2)	2.294(5)	Pt(1)–P(4)–Pt(2)	102.9(2)
Pt(2)–P(3)	2.339(5)	Cl(2)–Pt(2)–P(4)	160.6(2)
Pt(2)–P(4)	2.270(6)	Cl(2)–Pt(2)–P(3)	86.6(2)
P(2)–C(25)	1.75(2)	P(3)–Pt(2)–P(4)	103.6(2)
C(25)–C(30)	1.44(3)	P(2)–Pt(2)–P(3)	155.1(2)
		P(2)–Pt(2)–P(4)	90.7(2)
		Pt(2)–P(2)–C(25)	123.7(7)
		P(2)–C(25)–C(30)	121(2)
		C(25)–C(30)–Pt(1)	117(1)

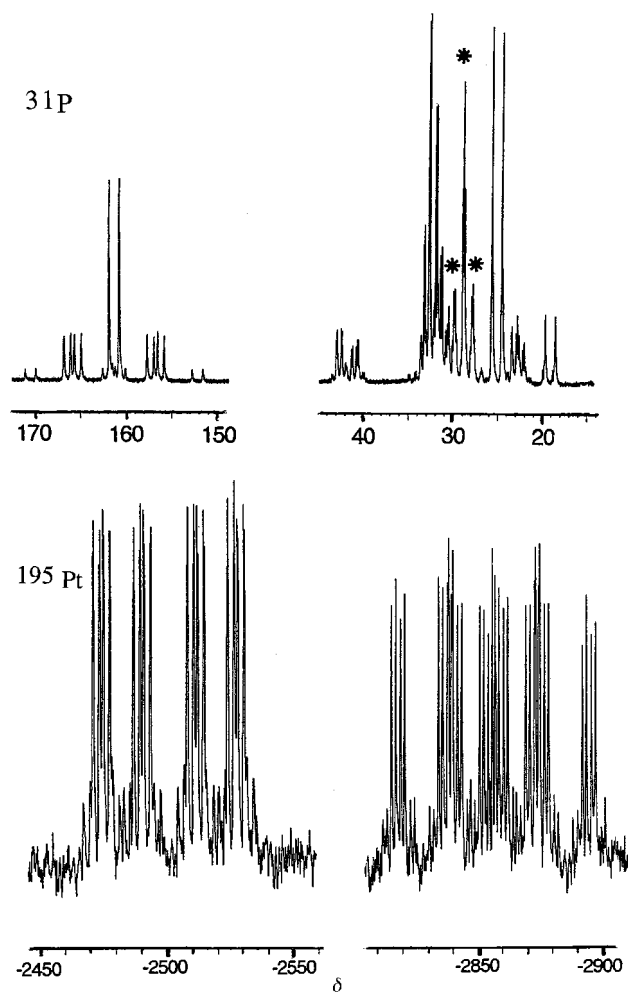


Fig. 5 The $^{195}\text{Pt}\text{-}\{^1\text{H}\}$ and $^{31}\text{P}\text{-}\{^1\text{H}\}$ NMR spectra (in acetone) of the cationic complex $[\text{Pt}_2\{\mu\text{-Au}(\text{PPh}_3)\}(\mu\text{-PPh}_2)\{\mu\text{-}(o\text{-C}_6\text{H}_4\text{PPh}_2)\}(\text{PPh}_3)_2]^+$ **6**. The asterisks denote the resonances of the P(5) nucleus bound to Au.

selected distances and angles are reported in Table 3. The Pt atoms, separated by 3.596(1) Å, each bear a terminal chloride ligand and are linked by two bridges, a μ -diphenylphosphido and an *ortho*-metallated $\mu\text{-}(o\text{-C}_6\text{H}_4\text{PPh}_2)$ ligand. These bridges form a six-membered boat-like ring with the two Pt atoms. The co-ordination geometry about Pt(1), defined by P(1), P(4), Cl(1) and C(30), is almost square planar with bond angles ranging from 86.1(6) to 95.4(3)°, whereas that about Pt(2), comprising P(2), P(3), P(4) and Cl(2), is best described as flattened tetrahedral. The mean planes of the two bridges are quasi-orthogonal. Compared with complex **3**, the PPh_2 bridge has been tilted by about 90° out of the molecular plane, and the two angles Pt(1)–P(4)–Pt(2) of the phosphido group and C(25)–

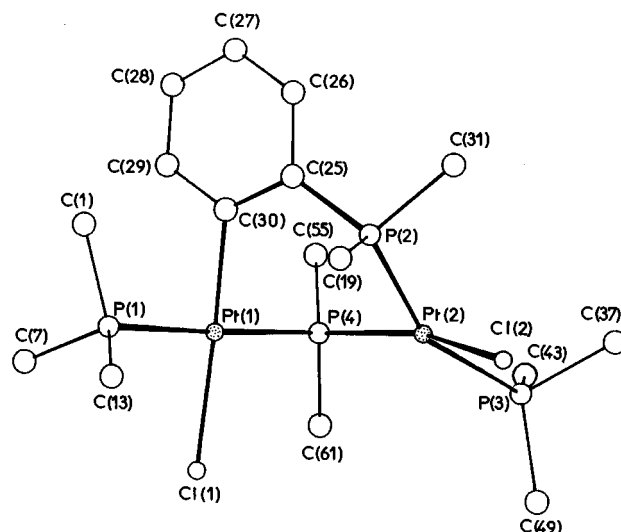


Fig. 6 View of the structure of $[\text{Pt}_2\text{Cl}_2(\mu\text{-PPh}_2)\{\mu\text{-}(o\text{-C}_6\text{H}_4\text{PPh}_2)\}(\text{PPh}_3)_2]^+$ **8**. For sake of clarity, the C_6H_5 groups bound to the phosphorus atoms are represented by their *ipso*-carbons only.

P(2)–Pt(2) in the cyclometallated ring have increased by 31.5 and 11.2° respectively. The flexibility of these fragments is well known and permits such variations.^{5,9,14,21} The “mixed geometry” exhibited here by the platinum centers imparts a grossly asymmetric overall structure to the complex.

NMR Spectroscopy

The $^{31}\text{P}\text{-}\{^1\text{H}\}$ NMR spectrum of complex **8** is very different from that of its precursor **3**. As a result of the opening of the Pt(1)–Pt(2)–P(4) ring the four signals of the phosphorus nuclei are grouped between δ 14.3 and 30.3. They form an ABMN spin system with complex satellites arising from isotopomers containing one or two ^{195}Pt nuclei, which give rise to ABMNX and ABMNX' systems, respectively. The derived P–P and Pt–P coupling constants are consistent with four phosphorus atoms being pairwise in *trans* position to each other with respect to two Pt^{II} (see Experimental section). The values for $^1J(\text{Pt}\text{-P})$ can be determined more precisely than in the ^{195}Pt NMR spectrum. Complex **8** exhibits a very simple ^{195}Pt NMR spectrum (Fig. 7): the signal of Pt(1) (δ –2459.3) is a ddd due to the coupling with P(1), P(2) and P(4), that of Pt(2) (δ –2956.8) appears as a doublet of triplets (linewidth 80 Hz), thus indicating that two of the three coupling constants of Pt(2) with the neighboring P atoms, P(2), P(3) and P(4), have very similar magnitudes. Each of the peaks is flanked by two satellites due to $J(\text{Pt}\text{-Pt}) = 198$ Hz. In view of the long separation between the platinum atoms this coupling must be considered as a ^{2+4}J passing through the bridges. All these data confirm the molecular structure established for **8** by X-ray diffraction (see Fig. 6).

The ^{195}Pt NMR spectrum of complex **8** always contained signals of two platinum atoms, in a 10% proportion, neighboring those of **8** and resembling them (see Fig. 7); ^{195}Pt resonances were thus observed at δ –2503 [ddd, $J(\text{Pt}\text{-Pt}) = ca. 400$, $J(\text{Pt}\text{-P}) = 2730, 2410, 480$ and 60] and –3018 [ddd, $J(\text{Pt}\text{-P}) = ca. 4100, 2130$ and 1930 Hz]. The similarity of their chemical shifts with those of **8** and their coupling constants $J(\text{Pt}\text{-Pt})$ and $J(\text{Pt}\text{-P})$ suggest the presence of a conformer of **8**, in which the geometry about the Pt would be slightly distorted. The flexibility of the skeleton ring could be favorable to the formation of such a conformer in solution. This phenomenon was not detected in the ^{31}P NMR spectrum.

The structures of complexes **1–3** show that the most evident results of the thermolysis of the platinum(0)–triphenylphosphine complexes are the cleavage of P–Ph and *ortho* C–H bonds and condensation of mononuclear fragments into di- and tri-nuclear clusters. Such transformations are well known

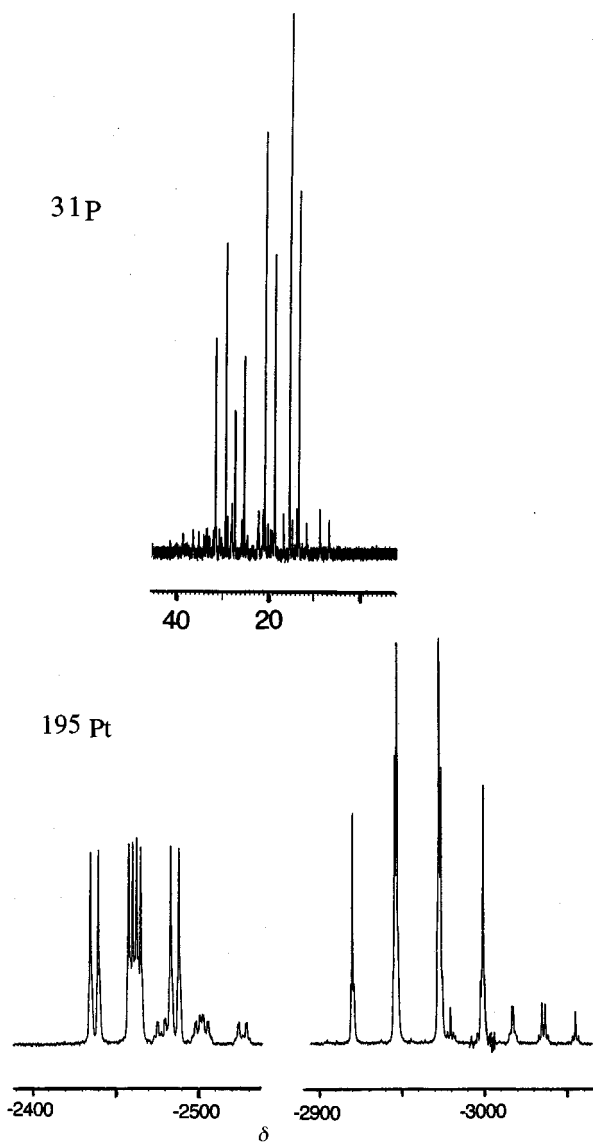


Fig. 7 The $^{195}\text{Pt}\{-^1\text{H}\}$ and $^{31}\text{P}\{-^1\text{H}\}$ NMR spectra (in CH_2Cl_2) of the complex $[\text{Pt}_2\text{Cl}_2(\mu\text{-PPh}_2)\{\mu\text{-}(o\text{-C}_6\text{H}_4\text{PPh}_2)\}(\text{PPh}_3)_2]$ **8**. For the small intensity peaks, see text.

and constitute often the route to the inactivation of organometallic catalysts;² but they permit also the synthesis of new compounds, inaccessible without this method.

Experimental

All experiments were performed under an inert atmosphere of deoxygenated and dried nitrogen with use of the Schlenk technique. All solvents were dried and distilled under nitrogen prior to use. Infrared spectra were measured in solid KBr on a Nicolet 205 FT-IR spectrometer and NMR spectra on Bruker AM 400 (^{31}P at 161.977 MHz) and ARX 500 spectrometer (^{31}P at 202.415 and ^{195}Pt at 107.315 MHz). The chemical shifts (δ) are given in ppm relative to external 85% H_3PO_4 for ^{31}P and to external Na_2PtCl_4 for ^{195}Pt . The spectra of these nuclei were ^1H decoupled. The complex $[\text{Pt}(\text{C}_2\text{H}_4)(\text{PPh}_3)_2]$ was prepared as described in the literature.²²

Preparations

[Pt₂{μ-PPh₂}{μ-(*o*-C₆H₄PPh₂)}(PPh₃)₂] **3**. Heating at 70 °C a 2-methoxyethanol solution (100 ml) of $[\text{Pt}(\text{C}_2\text{H}_4)(\text{PPh}_3)_2]$ (3.00 g, 4 mmol) under nitrogen for 4 h afforded, after cooling to room temperature, a red precipitate of the cluster $[\text{Pt}_3\text{Ph}(\mu\text{-PPh}_2)_3(\text{PPh}_3)_2]$ **2** (0.79 g). After filtration of this solid the filtrate

was evaporated to dryness and extraction of the residue with diethyl ether gave another red solid fraction of **2** (0.10 g). After evaporation of the diethyl ether of the extract, fractional recrystallization of the solid residue from CH_2Cl_2 -hexane (1 : 1) yielded pure yellow crystals of complex **3**. The mother-liquor of these crystals contained OPPh_3 and biphenyl mixed with a soluble fraction of **3**. Total yield of **2**: 0.89 g, 38%. Yield of **3**: 1.02 g, 37% (these yields are based on platinum) (Found: C, 58.2; H, 4.2. $\text{C}_{66}\text{H}_{54}\text{P}_4\text{Pt}_2$ **3** requires C, 58.2; H, 4.0%). IR (KBr pellet): $\nu(\textit{ortho}\text{-metallation})$ 725 cm^{-1} .

[Pt₂{μ-Cu(PPh₃)}(μ-PPh₂){μ-(*o*-C₆H₄PPh₂)}(PPh₃)₂]PF₆·4·PF₆. Complex **3** (0.14 g, 0.10 mmol) and $[\text{CuCl}(\text{PPh}_3)]$ (0.04 g, 0.11 mmol) were dissolved together in CH_2Cl_2 (10 ml). The salt TlPF_6 (0.04 g, 0.11 mmol) was added and the mixture stirred at room temperature for 3 h. After filtration of the white TlCl , layering of the filtrate with diethyl ether (20 ml) at -20 °C afforded yellow crystals of **4**· CH_2Cl_2 (yield: 0.115 g, 81%) (Found: C, 53.18; H, 3.86. $\text{C}_{85}\text{H}_{71}\text{Cl}_2\text{CuF}_6\text{P}_5\text{Pt}_2$ requires C, 53.26; H, 3.73%). IR (KBr pellet): $\nu(\textit{ortho}\text{-metallation})$ 724, $\nu(\text{PF}_6)$ 839 cm^{-1} .

[Pt₂{μ-Ag(PPh₃)}(μ-PPh₂){μ-(*o*-C₆H₄PPh₂)}(PPh₃)₂]NO₃·5·NO₃. A mixture of complex **3** (0.14 g, 0.10 mmol) and $[\text{Ag}(\text{PPh}_3)]\text{NO}_3$ (0.044 g, 0.10 mmol) in CH_2Cl_2 (10 ml) was stirred at room temperature for 30 min. Addition of diethyl ether (30 ml) and cooling at -20 °C afforded orange crystals of **5**·0.5 CH_2Cl_2 . Yield: 0.17 g, 92% (Found: C, 55.31; H, 3.76; N, 0.57. $\text{C}_{85.5}\text{H}_{70}\text{AgClNO}_3\text{P}_5\text{Pt}_2$ requires C, 55.28; H, 3.84; N, 0.76%). IR (KBr pellet): $\nu(\textit{ortho}\text{-metallation})$ 724, $\nu(\text{NO}_3)$ 1386, 1343 cm^{-1} .

[Pt₂{μ-Au(PPh₃)}(μ-PPh₂){μ-(*o*-C₆H₄PPh₂)}(PPh₃)₂]PF₆·6·PF₆. A mixture of complex **3** (0.14 g, 0.10 mmol), $[\text{AuCl}(\text{PPh}_3)]$ (0.05 g, 0.10 mmol) and TlPF_6 (0.04 g, 0.11 mmol) in CH_2Cl_2 (20 ml) was stirred at room temperature for 2 h. After filtration of the white TlCl , diethyl ether (40 ml) was added to the filtrate and cooling at -20 °C afforded orange crystals of **6** (yield 0.147 g, 76%) (Found: C, 52.55; H, 3.88. $\text{C}_{84}\text{H}_{69}\text{AuF}_6\text{P}_6\text{Pt}_2$ requires C, 52.15; H, 3.59%). IR (KBr pellet): $\nu(\textit{ortho}\text{-metallation})$ 725, $\nu(\text{PF}_6)$ 840 cm^{-1} .

[Pt₂Cl₂(μ-PPh₂){μ-(*o*-C₆H₄PPh₂)}(PPh₃)₂] **8**. Solid HgCl_2 (0.03 g, 0.10 mmol) was added to a solution of complex **3** (0.14 g, 0.10 mmol) in CH_2Cl_2 (15 ml). The mixture turned red and, after 15 min stirring at room temperature, was filtered and concentrated *in vacuo* to ca. 10 ml. Layering with hexane (20 ml) and standing at room temperature for 2 h precipitated mercury metal. After filtration and concentration to half the volume, complex **8** crystallized out as yellow crystals, suitable for X-ray diffraction studies (yield: 0.13 g, 85%) (Found: C, 55.47; H, 3.78. $\text{C}_{66}\text{H}_{54}\text{Cl}_2\text{P}_4\text{Pt}_2$ requires C, 55.35; H, 3.80%). IR (KBr pellet): $\nu(\textit{ortho}\text{-metallation})$ 725 cm^{-1} . NMR data: ^{195}Pt ($\text{CH}_2\text{Cl}_2\text{-CD}_2\text{Cl}_2$), δ -2459 {ddd, Pt(1), $J[\text{Pt}(1)\text{Pt}(2)] = 198$, $^1J[\text{Pt}(1)\text{P}(1)] = 2737$, $^1J[\text{Pt}(1)\text{P}(4)] = 2472$, $^3J[\text{Pt}(1)\text{P}(3)] = 517$ } and -2957 {ddd, Pt(2), $^1J[\text{Pt}(1)\text{Pt}(2)] = 198$, $^1J[\text{Pt}(2)\text{P}(2)] = 2878$, $^1J[\text{Pt}(2)\text{P}(3)] = 2850$, $^1J[\text{Pt}(2)\text{P}(4)] = 2728$ Hz}; $^{31}\text{P}\{-^1\text{H}\}$ ($\text{CH}_2\text{Cl}_2\text{-CD}_2\text{Cl}_2$), δ 14.3 {d, P(1), $^1J[\text{P}(1)\text{Pt}(1)] = 2735$, $^2J[\text{P}(1)\text{P}(4)] = 412$ }, 19.4 {dd, P(2), $^1J[\text{P}(2)\text{Pt}(2)] = 2880$, $^2J[\text{P}(2)\text{P}(3)] = 442$, $^2J[\text{P}(2)\text{P}(4)] = 5$ }, 26.3 {ddd, P(4), $^1J[\text{P}(4)\text{Pt}(2)] = 2740$, $^1J[\text{P}(4)\text{Pt}(1)] = 2482$, $^2J[\text{P}(1)\text{P}(4)] = 412$, $^2J[\text{P}(2)\text{P}(4)] = 5$, $^2J[\text{P}(3)\text{P}(4)] = 17.5$ } and 30.3 {dd, P(3), $^1J[\text{P}(3)\text{Pt}(2)] = 2850$, $^3J[\text{P}(3)\text{Pt}(1)] = 517$, $^2J[\text{P}(2)\text{P}(3)] = 442$, $^2J[\text{P}(3)\text{P}(4)] = 17.5$ Hz}.

Crystal structure determinations

Single crystals of complex **3** were grown by slow diffusion of water into a concentrated acetone solution. Suitable single crystals of **3**· CH_2Cl_2 were grown by slow diffusion of pentane into a CH_2Cl_2 solution of **3**. Crystal data and details of meas-

Table 4 Crystal data and data collection for [Pt₂(μ-PPh₂){μ-(*o*-C₆H₄PPh₂)}(PPh₃)₂] **3**, **3**·CH₂Cl₂ and [Pt₂Cl₂(μ-PPh₂){μ-(*o*-C₆H₄PPh₂)}(PPh₃)₂] **8**

	3	3 ·CH ₂ Cl ₂	8
Formula	C ₆₆ H ₅₄ P ₄ Pt ₂	C ₆₇ H ₅₆ Cl ₂ P ₄ Pt ₂	C ₆₆ H ₅₄ Cl ₂ P ₄ Pt ₂
<i>M</i>	1361.24	1446.17	1432.15
Crystal system	Monoclinic	Monoclinic	Monoclinic
Space group	<i>P</i> ₂ / <i>c</i> (<i>C</i> 52 <i>h</i>)	<i>P</i> ₂ / <i>c</i> (no. 14)	<i>C</i> 2/ <i>c</i> (<i>C</i> 62 <i>h</i>)
Crystal dimensions/mm	0.20 × 0.15 × 0.20	0.20 × 0.15 × 0.20	0.10 × 0.20 × 0.20
Crystal color and habit	Pale orange pinacoid + prism	Orange prism	Yellow pinacoid + prism
<i>a</i> /Å	14.385(3)	14.347(4)	28.643(3)
<i>b</i> /Å	22.298(6)	13.471(1)	10.751(3)
<i>c</i> /Å	17.391(9)	29.939(1)	39.670(6)
β/°	97.94(3)	91.39(1)	93.54(1)
<i>U</i> /Å ³	5525	5784.8	12193
<i>Z</i>	4	4	8
<i>D</i> _c /g cm ⁻³	1.62	1.666	1.56
<i>F</i> (000)	2664	2832	5600
Radiation	Ag-Kα ₁	Mo-Kα ₁	Mo-Kα ₁
(graphite monochromator)	(λ = 0.55941 Å)	(λ = 0.71073 Å)	(λ = 0.70930 Å)
μ/cm ⁻¹	29.0	51.23	50.5
θ Limits/°	1–20	2–30	2–27
Octants collected	<i>h</i> , <i>k</i> ± <i>l</i>	<i>h</i> , – <i>k</i> , ± <i>l</i>	± <i>h</i> , <i>k</i> , <i>l</i>
No. data collected	8640	10800	13400
No. unique data used [<i>I</i> > 3σ(<i>I</i>)]	3094	6851	4450
No. variables	649	676	667
<i>R</i>	0.056	0.036	0.058
<i>R</i> '	0.059	0.049	0.044
Goodness of fit	0.72	1.54	2.62
Largest peak in final difference map/e Å ⁻³	1	1.19	1

Measurements for compounds **3**, **3**·CH₂Cl₂ and **8** are given in Table 4. Data for all structures were collected at 20 °C on an Enraf-Nonius CAD-4 diffractometer. Data reduction was made by using the SDP package with a decay correction.²³ The structures were solved by standard direct methods of phase determination and Fourier methods.²⁴ Empirical absorption corrections were applied using DIFABS.²⁵ All non-hydrogen atoms were located and refined anisotropically. The hydrogens were placed in calculated positions and included in the refinement with a fixed isotropic thermal parameter of 5 Å². Full-matrix least-squares refinements led to the final agreement factors given in Table 4. Atomic scattering factors and anomalous dispersion corrections were taken from standard sources.^{23,26}

CCDC reference number 186/1321.

Acknowledgements

We thank D. Bayeul (Nancy) for his contribution to the structural determinations and Professor P. Granger (Université Louis Pasteur) for his support of the NMR studies. We are grateful to the Centre National de la Recherche Scientifique, the Ministère de l'Éducation Nationale, de l'Enseignement Supérieur et de la Recherche, the Ministère des Affaires Étrangères (Paris) and the Ministère des Affaires Étrangères (Alger) for support of the Strasbourg-Constantine Cooperation Project 96 MDU 371.

References

- 1 L. Malatesta and M. Angoletta, *J. Chem. Soc.*, 1957, 1186; L. Malatesta and C. Cariello, *J. Chem. Soc.*, 1958, 2323.
- 2 P. E. Garrou, *Chem. Rev.*, 1985, **85**, 171.
- 3 N. J. Taylor, P. C. Chieh and A. J. Carty, *J. Chem. Soc., Chem. Commun.*, 1975, 448.
- 4 R. Bender, P. Braunstein, A. Tiripicchio and M. Tiripicchio Camellini, *Angew. Chem., Int. Ed. Engl.*, 1985, **24**, 861.
- 5 R. Bender, P. Braunstein, A. Dedieu, P. D. Ellis, B. Higgins, P. D. Harvey, E. Sappa and A. Tiripicchio, *Inorg. Chem.*, 1996, **35**, 1223.
- 6 O. J. Scherer and K. Hussong, personal communication.
- 7 R. Bender, C. Archambault and P. Braunstein, Xth FEChem Conference on Organometallic Chemistry, Agia Pelagia, Crete (Greece), 5–10 September, 1993, Abstract P45.
- 8 C. Archambault, R. Bender, P. Braunstein, A. DeCian and J. Fischer, *Chem. Commun.*, 1996, 2729.
- 9 M. A. Bennett, D. E. Berry, S. K. Bhargava, E. J. Ditzel, G. B. Robertson and A. C. Willis, *J. Chem. Soc., Chem. Commun.*, 1987, 1613.
- 10 D. M. Blake and C. J. Nyman, *Chem. Commun.*, 1969, 483. Note however that in their full paper these authors did not confirm the presence of a cyclometallated ligand: D. M. Blake and C. J. Nyman, *J. Am. Chem. Soc.*, 1970, **92**, 5359.
- 11 F. Glockling, T. McBride and R. J. I. Pollock, *J. Chem. Soc., Chem. Commun.*, 1973, 650.
- 12 S. Sostero, O. Traverso, M. Lenarda and M. Graziani, *J. Organomet. Chem.*, 1977, **134**, 259.
- 13 H. C. Clark and K. E. Hine, *J. Organomet. Chem.*, 1976, **105**, C32.
- 14 D. P. Arnold, M. A. Bennett, M. S. Bilton and G. B. Robertson, *J. Chem. Soc., Chem. Commun.*, 1982, 115.
- 15 M. A. Bennett, D. E. Berry, T. Dirnberger, D. C. R. Hockless and E. Wenger, *J. Chem. Soc., Dalton Trans.*, 1998, 2367.
- 16 R. Bender and P. Braunstein, unpublished results.
- 17 *Phosphorus-31 NMR Spectroscopy in Stereochemical Analysis*, VCH, Weinheim, 1987, p. 559.
- 18 R. Bender, P. Braunstein, A. Dedieu and Y. Dusausoy, *Angew. Chem., Int. Ed. Engl.*, 1989, **28**, 923.
- 19 P. R. Sharp, *Inorg. Chem.*, 1986, **25**, 4185.
- 20 P. Braunstein, M. Ries, C. de Méric de Bellefon, Y. Dusausoy and J.-P. Mangeot, *J. Organomet. Chem.*, 1988, **355**, 533.
- 21 M. A. Bennett, S. K. Bhargava, D. C. Hockless, L. L. Welling and A. C. Willis, *J. Am. Chem. Soc.*, 1996, **118**, 10469.
- 22 U. Nagel, *Chem. Ber.*, 1982, **115**, 1998.
- 23 SDP Structure Determination Package, Enraf-Nonius, Delft, 1977.
- 24 G. M. Sheldrick, Programs for Crystal Structure Determination, University of Göttingen, 1976.
- 25 N. Walker and D. Stuart, *Acta Crystallogr., Sect. A*, 1983, **39**, 159.
- 26 *International Tables for X-Ray Crystallography*, Kynoch Press, Birmingham, 1974, vol. IV.

Paper 8/09448I